3151

NUREG/CR-0481
SAND77-1872
R-7

An Assessment of Stress-Strain Data Suitable for Finite-Element Elastic-Plastic Analysis of Shipping Containers

Henry J. Rack, Gerald A. Knorovsky

Sandia Laboratories

Prepared for

U. S. NUCLEAR REGULATORY COMMISSION

NUREG/CR-0481
SAND77-1872
R-7

AN ASSESSMENT OF STRESS-STRAIN DATA SUITABLE FOR FINITE-ELEMENT ELASTIC-PLASTIC ANALYSIS OF SHIPPING CONTAINERS

H. J. Rack
G. A. Knorovsky

Date Published: September 1978

APPROVED:

Manager, Nuclear Fuel Cycle Technology Development

Director, Nuclear Fuel Cycle Programs

Sandia Laboratories
Albuquerque, New Mexico 87185

Operated by
Sandia Corporation
for the
U. S. Department of Energy

Prepared for
Division of Safeguards, Fuel Cycle and Environmental Research
Office of Nuclear Regulatory Research
U. S. Nuclear Regulatory Commission
Under Interagency Agreement DOE 40-550-75
NRC FIN No. A1045

ABSTRACT

Stress-strain data which describes the influence of strain rate and temperature on the mechanical response of materials presently being used for light water reactor shipping containers have been assembled. Selection of data has been limited to that which is suitable for use in finite-element elastic-plastic analysis of shipping containers (e.g., they must include complete material history profiles). Based on this information, recommendations have been made for further work which is required to complete the necessary data base.

CONTENTS

TABLES

ILLUSTRATIONS

ILLUSTRATIONS (cont.)

ILLUSTRATIONS (cont.)

AN ASSESSMENT OF STRESS-STRAIN DATA SUITABLE FOR FINITE-ELEMENT ELASTIC-PLASTIC ANALYSIS OF SHIPPING CONTAINERS

Introduction

Recent progress in finite-element elastic-plastic analysis has brought with it a requirement for a more detailed description of a material's response to imposed mechanical and thermal loadings. Unfortunately, metallurgists have in the past typically reported the influence of such variables as temperature and strain rate only on selected properties (e.g., yield strength or tensile elongation) rather than the generalized elastic-plastic representation required for modern computer program applications.

Notwithstanding this shortcoming, a body of literature exists that can form the basis for advanced computer-aided design. The purpose of this report is to assess and compile available data, particularly those relevant to materials which are being used for light water reactor (LWR) spent fuel shipping container primary structures. Consequently, this assessment has been limited to selected stainless steels, uranium, and chemical lead. It includes, where possible, data on the stress-strain behavior of these materials over a range of strain rates (10^{-5} to 10^{2} sec^{-1}) and temperatures (-40 to 320°C; -40°F to 620°F) thought to be typical of shipping cask environments.

This survey has considered only uniaxial deformation, tensile or compressive, and does not contain any multiaxial information. In addition, fracture, creep, and cyclic loading conditions have been excluded. Since the data sources examined in

BLANK PAGE

this study generally did not cite whether the values given were average or minimum data reported are thought to be typical of the materials being examined rather than representing either average or minimum values.

This report first lists the materials used in typical shipping cask designs and their procurement specifications. It then discusses the available mechanical properties data, particularly stress-strain curves, treating each of the specific materials in separate subsections. Finally, the report recommends specific areas for further research and data acquisition.

Materials

Table I lists the chemical compositions of some of the materials presently used for LWR shipping casks. Table II lists the specific cask being considered and the material specification required for procurement of the requisite structural shapes.

Mechanical Properties

Austenitic Stainless Steels

Many investigators have examined austenitic stainless steels, because of their excellent corrosion resistance, creep resistance, and high toughness. However, their studies have tended to neglect the regime of stress/strain-rate/temperature of interest for shipping cask applications.

Probably the most extensive compilation of stress-strain data may be found in studies conducted at the Oak Ridge National

TABLE I

Chemical Composition of LWR Shipping Cask Materials
(percentage by weight; maximum amount unless otherwise noted)

	C	Mn	Si	P	S	Cr	Ni	Mo	Other
Austenitic									
216	0.08	7.5 -9.0	1.0	0.045	0.03	17.5 -22.0	5.0 - 7.0	1.0 -3.0	0.25/.5 N
304	0.08	2.0	1.0	0.045	0.03	18.0 -20.0	8.0-10.5		
304L	0.03	2.0	1.0	0.045	0.03	18.0 -20.0	8.0-12.0		
308	0.08	2.0	1.0	0.045	0.03	19.0 -21.0	10.0-12.0		
316	0.08	2.0	1.0	0.045	0.03	16.0 -18.0	10.0-14.0	2.0 -3.0	
317	0.08	2.0	1.5	0.040	0.04	18.0 -21.0	9.0-13.0	3.0 -4.0	
321	0.08	2.0	1.0	0.045	0.03	17.0 -19.0	9.0-12.0		0.7 Ti
347	0.08	2.0	1.0	0.045	0.03	17.0 -19.0	9.0-13.0		1.1 (Ta+Cb)
Ferritic									
A333 Gr 1	0.03	0.4- 1.06	-	0.04	0.06	- - 0.65	- 0.7- 1.0	0.4 -0.6	-
A516 (5-1)	0.1 -0.2	0.6- 1.0	0.15-0.35	0.035	0.04				0.03/0.08 V|0.002/ 0.006 B|0.15/0.5 Cu
A516 Gr 55 1/2"	0.18	0.56-0.94	0.13-0.33	0.035	0.04				
2"	0.2	0.56-1.25	0.13-0.33	0.035	0.04				
4"	0.22	0.56-1.25	0.13-0.33	0.035	0.04				
8"	0.24	0.56-1.25	0.13-0.33	0.035	0.04				
A516 Gr 70 1/2"	0.2	0.56-1.25	0.13-0.33	0.035	0.04				
2"	0.27	0.8 - 1.25	0.13-0.33	0.035	0.04				
4-8"	0.28	0.56-1.25	0.13-0.33	0.035	0.04				
	0.30	0.8 - 1.25	0.13-0.33	0.035	0.04				
A350	0.31	0.8 - 1.25	0.13-0.33	0.035	0.04				
A203	0.30-0.43	0.75-1.0	0.28-0.55	0.025	0.025	0.8 - 1.1	0.25	0.15-0.25	0.25 Cu
A203	0.45-0.65	0.75-1.0	0.28-0.55	0.025	0.025	0.8 - 1.1	0.25	0.15-0.25	0.25 Cu
A350	0.45-0.65	0.75-1.0	0.28-0.55	0.025	0.025	0.8 - 1.1	0.25	0.15-0.25	0.25 Cu
A350	0.30-0.43	0.6 -0.85	0.2 -0.35	0.04	0.04	0.7 - 0.9	1.6 - 2.0	0.2 -0.3	-
Precipitation Hardening									
17-4 PH	0.04	0.4	0.3	- -	- -	15.3	4.25	-	0.25 Cb|3.6 Cu
A564 630 (630)	0.05	1.35	0.3	- -	- -	15.5 -16.8	24.0 -27.0	1.0 -1.5	1.0|2.35 Ti| 0.25 A|0.3 V
	Cu	Mn	Si	Fe	Zn	Cr	Mg	Si	
Aluminum									
1100	0.01	-	0.09	0.09	0.1	-	-	0.02	
3003	0.05-0.2	1.0 -1.5	0.6	0.7	0.25	0.04-0.35	0.8 - 1.2	-	- - - -
6061	0.15-0.4	0.15	0.4 -0.8	0.7	0.25	0.17	0.45- 0.8	0.15	
6063	0.10	0.10	0.2 -0.6	0.35	0.1	0.10-0.35	0.45 - 0.9	0.1	
7075	0.10	0.10	-	-	-	-	2.1 - 2.9	-	0.045 (Ti+Zr)
Chemical Fe	0.04-0.08	-	- -	0.004	0.001	- -	- -	- -	0.005 B|0.002/ 0.02 Zr|0.002

TABLE II

Material Procurement Specifications for Light Water Reactor Shipping Casks

Cask	Material	Specification*	Form
NFS-4, NFS-5	304	-	plate, sheet, forging
Spent Fuel Shipping Cask	321		
	347		
	Boltz Cd Plated	A325	bolts
	Pb	B29	shielding
	B-28Bo	-	shielding
IF 300	216	A240	sheet, plate
	304	A182,A240,A351	forging, casting, sheet, plate
	316	-	valve coupling
	317	A296Gr	cast form
	A514	A514	plate
	A516	A516	plate
	4340	-	bar
	17-4 PH	-	steel, wire
	3003 Al	-	sheet, plate
	6061 Al	-	sheet, plate
	6063 Al	-	sheet, plate
	Pb	B29	shielding
NL 10/24 Rail Cask	304	A240,A312,A336, A182,A269	sheet, plate, forging
	4140, 4142, 4145	A193	bolting
	17-4 PH	-	pipe & fittings, tubing
	660 (A286)	A453	bolting
	1100 Al, 5052-H32	-	-
	Pb	B29	shielding
	B	NLI 7065 #1	neutron shield
	Ag-In-Cd	-	neutron absorber
TN 8, TN 9	304	SA320 B8	bolts
	304L	-	plate, sheet, forgings
	A333	A333 gr 55	pipe
	A516	A516 gr 55	plate
	4140, 4142, 4145	SA320 L7	bolting
	4340	SA320 L43	bolting
	Pb	B29	shielding
	Cu 1/2 hard	B152	plate

* Refers to SAE or ASTM specification (with the exception of the NL specification for U).
**Includes additional composition restrictions imposed by manufacturer.

Laboratory and the Hanford Engineering Development Laboratory. Since these examinations were in support of the LMFBR program, they have been principally concerned with temperatures above those of concern to this program. Table III summarizes the applicable data banks presently available from these institutions. These investigators have shown that while the yield strength of 304 stainless steel at 25°C (77°F) increases by 48 MN/m^2 per decade increase in strain rate, the overall stress-strain behavior of the alloy does not appear to be radically altered by these rate changes.

The stress-strain curves shown in Figures 1 through 6 and Table IV should be considered only as typical of the respective alloys and product forms. Studies [3] of different product forms produced from a single heat of 304 stainless steel have demonstrated that even when chemistry variables are eliminated, variations in processing operations can cause large changes in the stress-strain response. This effect of processing variations is further complicated by the rather wide chemistry allowables shown in Table I. Combinations of these factors--different chemistry and processing--have led to considerable property variability for nominally identical alloys. Examples of this heat-to-heat variability are given in Figures 7 and 8 for 304 and 316 stainless steels, respectively.

Two additional phenomena, (i.e., the formation of deformation induced martensite and dynamic strain-aging) have been observed during tensile straining of austenitic stainless steels. The former can result in drastic changes in the stress-strain

TABLE III

Stress-Strain Curve Availability for Selected Stainless Steels*

	Strain Rate (sec^{-1})									
Temperature, °C(°F)	$3x10^{-6}$	$8x10^{-6}$	$4x10^{-5}$	$7x10^{-5}$	$8x10^{-5}$	$4x10^{-4}$	$7x10^{-4}$	$8x10^{-4}$	$8x10^{-3}$	$7x10^{-1}$
25 (77)	-	304	304	304§	304	304	304	304	304	304§
	-	-	308	-	-	308	304§	-	-	-
	-	-	308L	316	-	308CRE	316¶	-	-	-
	-	-	308+	-	-	308§	316	-	-	-
	-	-	308CRE	-	-	308CRE§	-	-	-	-
	-	-	-	-	-	304§	-	-	-	-
93 (200)	-	-	-	-	304	304	316	-	304	-
	-	-	-	316	-	-	-	-	-	-
204 (400)	304	-	-	304§	304	316	-	-	304	-
	-	-	-	316	-	304	-	-	-	-
260 (500)	-	-	-	-	-	-	-	304	-	-
300 (575)	-	-	304	304§	-	-	-	-	-	-
316 (600)	304	-	308	316	304	304	316	304	304	-
	-	-	308+	-	308	-	-	-	-	-
	-	-	308L	-	308CRE	-	-	-	-	-
	-	-	308L+	-	-	-	-	-	-	-
	-	-	308	-	-	-	-	-	-	-

*All 308 variations are weld metal.
+Irradiated
§Aged (various treatments)
¶Weld Material

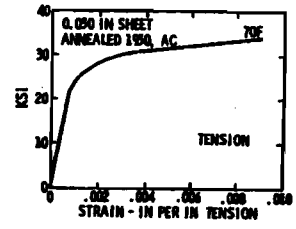

Figure 1. Stress-strain curves for 321 stainless steel sheet at room temperature [13].

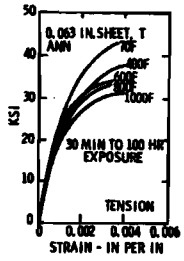

Figure 2. Compressive stress-strain curves for 321 stainless steel sheet at room and elevated temperatures [1].

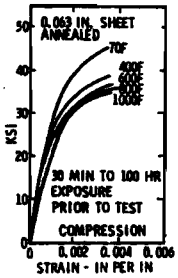

Figure 3. Stress-strain curves for 321 stainless steel sheet at room and elevated temperatures [1].

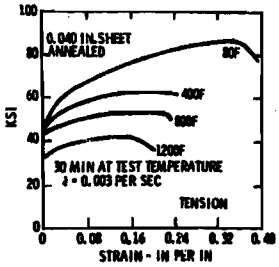

Figure 4. Stress-strain curves for 321 stainless steel sheet at room and elevated temperatures [1].

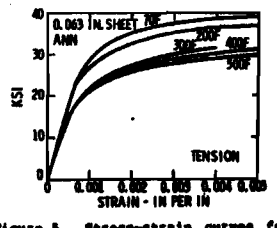

Figure 5. Stress-strain curves for 347 stainless steel sheet at room and elevated temperatures [1].

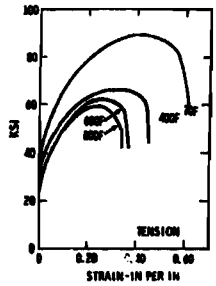

Figure 6. Stress-strain curves to failure at room and elevated temperatures for 347 stainless steel [1].

TABLE IV

Tensile Properties of Representative Stainless Steel Alloys

	Test Temperature °C	-50	-20	0	20	100	200	300	400
	Tensile Strength ksi	159.7	141.6	127.4	89.6	68.8	63.4	63.2	63.2
	Stress ksi @								
Type	0.02% Strain	24.6	28.0	28.7	28.2	19.7	15.2	14.3	12.8
304	0.05% Strain	28.7	31.4	31.8	30.0	21.5	17.9	16.6	15.5
	0.1 % Strain	33.8	33.2	33.6	31.4	22.8	19.0	17.7	16.6
	0.2 % Strain	34.3	34.9	35.2	32.7	24.2	20.2	18.8	17.5
	Elongation (%)	56.1	55.9	64.7	70.8	58.5	49.1	44.7	45.5
	Reduction of Area (%)	71.0	67.0	75.0	77.4	78.5	75.2	69.6	72.0
	Tensile Strength ksi	120.7	104.8	98.6	84.7	72.1	66.8	67.2	67.6
	Stress ksi @								
	0.02% Strain	37.2	33.6	30.2	28.7	22.0	18.6	17.5	16.1
Type	0.05% Strain	42.3	37.6	33.8	30.9	24.0	19.9	18.4	17.0
316	0.1 % Strain	45.2	39.9	36.7	32.3	25.5	20.8	19.0	17.7
	0.2 % Strain	48.8	41.7	37.9	34.0	26.7	22.0	20.2	18.8
	Elongation (%)	84.0	87.3	80.1	60.7	54.1	48.2	45.5	45.6
	Reduction of Area (%)	74.0	74.0	62.0	77.4	76.3	75.2	68.4	69.6
	Tensile Strength ksi	147.6	127.7	110.4	85.8	71.5	63.8	60.9	62.9
	Stress ksi @								
	0.02% Strain	22.8	27.6	34.0	22.8	18.8	19.0	15.7	14.1
Type	0.05% Strain	26.7	30.9	39.4	25.5	23.3	20.8	17.7	16.6
321	0.1 % Strain	30.0	33.2	40.5	27.3	25.1	22.2	19.3	17.7
	0.2 % Strain	34.5	36.1	41.0	29.3	26.7	23.5	20.4	20.2
	Elongation (%)	47.6	53.5	64.2	63.8	53.7	45.0	39.7	39.4
	Reduction of Area (%)	70.0	71.7	75.0	7..4	78.4	72.0	72.0	67.2
	Tensile Strength ksi	145.6	127.2	111.6	94.3	75.5	66.5	64.1	64.5
	Stress ksi @								
	0.02% Strain	29.3	30.7	29.8	29.8	23.1	19.3	17.9	17.5
Type	0.05% Strain	34.9	35.8	32.9	31.4	25.8	23.3	20.2	19.3
347	0.1 % Strain	39.4	39.2	37.9	33.2	27.8	25.3	22.4	20.4
	0.2 % Strain	44.8	42.8	40.1	35.2	29.3	27.1	23.7	22.0
	0.5 % Strain	48.8	45.2	41.0	35.8	-	-	-	-
	1.0 % Strain	52.4	50.2	43.7	38.8	-	-	-	-
	Elongation (%)	49.5	56.2	65.2	54.6	48.0	41.1	41.3	39.3
	Reduction of Area (%)	69.6	64.0	75.0	72.0	65.8	72.0	70.0	67.2

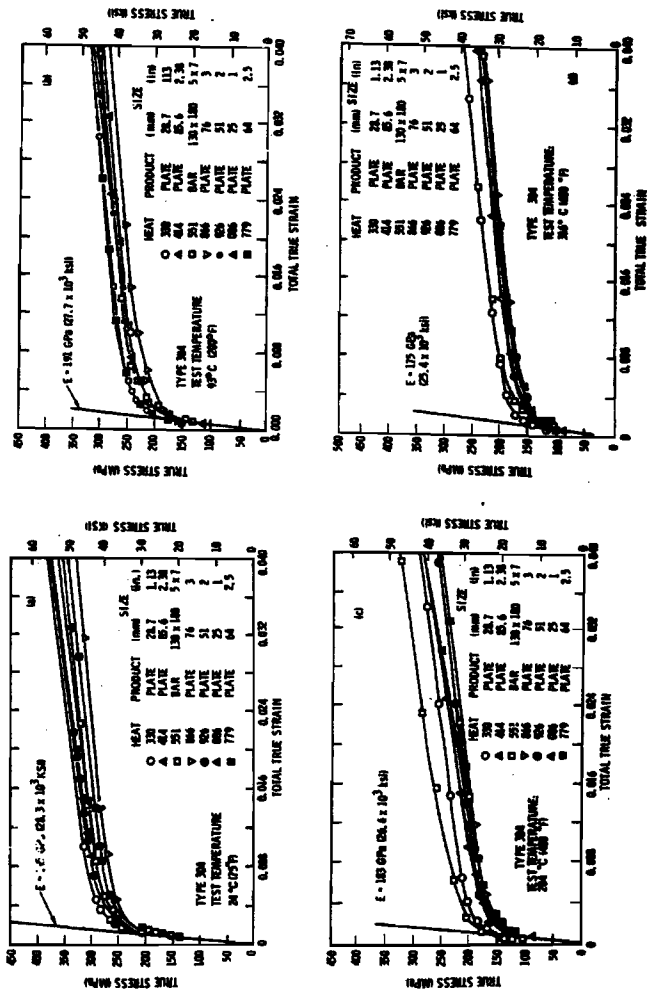

Figure 7. Heat-to-heat variation in stress-strain diagram for 304 stainless steel tested at (a) 24°C, (b) 93°C, (c) 204°C, and (d) 316°C [4].

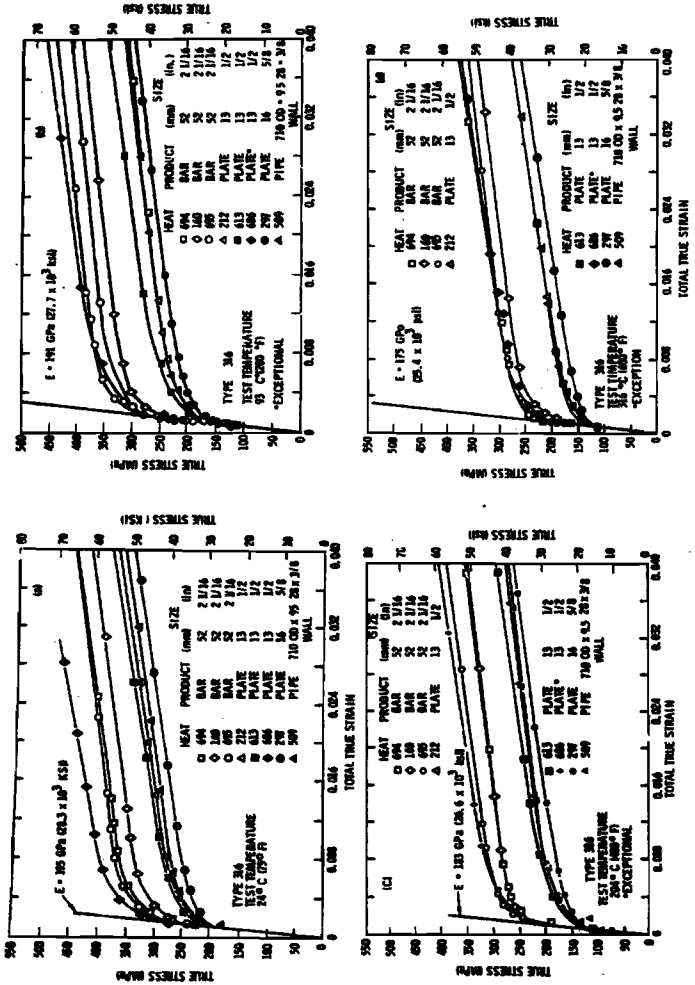

Figure 8. Heat-to-heat variation in stress-strain diagrams for 316 stainless steel at (a) 24°C, (b) 93°C, (c) 204°C, and (d) 316°C [4].

behavior. Figure 9 shows a representative example of the effect of test temperature on the mechanical response of 301, an alloy less stable (i.e., more prone to martensite formation) than 304. Normally, stable austenitic stainless steels show an increase in yield and ultimate strengths with decreasing temperatures below ambient [2]. On the other hand, martensite-forming grades exhibit a slight decrease in yield but a rapid increase in ultimate strength. A sharp maxima in the tensile ductility also occurs (Figures 10 and 11). Although austenitic stainless steels (such as 304) which are used for LWR shipping casks are typically thought to be quite stable with respect to martensite formation, it is possible this transformation might occur in containers stressed at low temperatures. Unfortunately, the

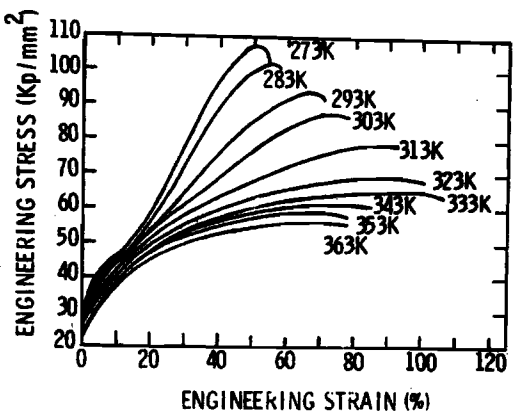

Figure 9. Engineering stress versus engineering strain for the 301 stainless steel tested at a strain rate of 1.03 x 10^{-3} sec^{-1} [5].

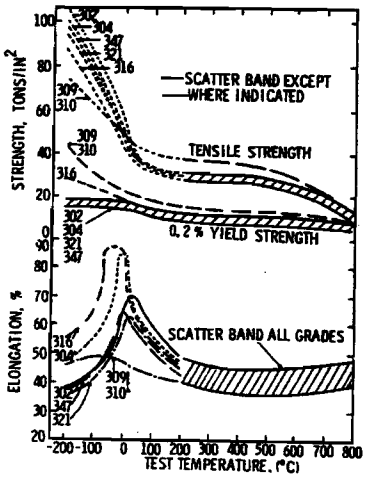

Figure 10. Tensile properties of standard grades of austenitic steel in temperature range -200 to +800°C [2].

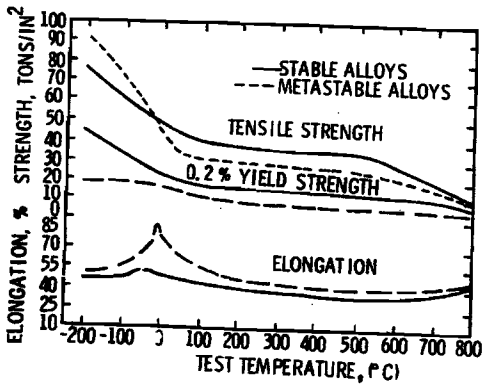

Figure 11. Effect of alloy stability on tensile properties of austenitic steels [2].

importance of this phenomenon cannot be quantitatively assessed at this time.

Dynamic strain-aging, the second phenomenon alluded to above, is usually associated with a change in the strain rate sensitivity (i.e., from an increase in flow stress with increasing strain rate to a decrease). Many consider strain-aging to be limited to bcc metals. There is evidence, however, that austenitic stainless steels may also exhibit dynamic strain-aging (serrations in the stress/strain curve) particularly in the temperature range 200 to 700°C [6]. The cross-hatched area in Figure 12 indicates the temperature and strain-rate regime within

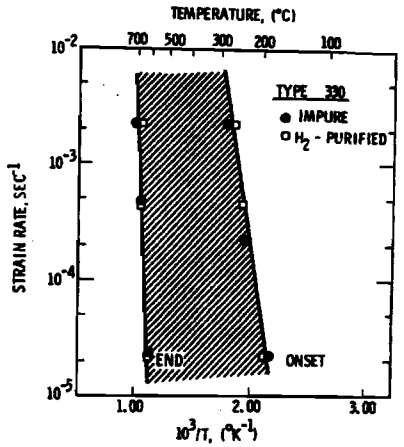

Figure 12. Relationship between strain rate and temperature for serrated flow in type 330 stainless steel [6].

which serrated flow is encountered in an AISI 330 stainless steel (Fe-15Cr-35Ni). In a more limited investigation [7], serrations have been reported in a type 316 stainless steel tested at 200°C utilizing a strain rate of $1.3 \times 10^{-2} sec^{-1}$. These conditions correspond with those predicted from the diagram for type 330 stainless steel.

The effect of strain-aging may also be important in weld regions. Current practice involves preparation of weldments with a small percentage (< 10 percent) of body-centered cubic (bcc) ferrite. This raises the possibility that not only might dynamic strain-aging take place in the face-centered cubic (fcc) parent (base) metal but also in the partially bcc weld region, perhaps under different conditons of temperature and strain-rate.

Finally, it should be recognized that it is virtually impossible to gather enough data to describe every conceivable combination of strain-rate and temperature. For this reason, procedures for interpolation and extrapolation between a more reasonable number of data points are required. Indeed, the ideal situation would be to obtain an accurate "equation of state" which might allow one to dispense with or minimize the requirements for a data bank. Some progress has been made toward this goal [8-11]. These attempts involve parameterization of the stress/strain curves with the aim of reporting the influences of strain-rate, temperature, and material history on these characteristic functions. Some proposed equations are shown in Table V. However, these representations all suffer from a number of common difficulties. For example, none can predict the strain

TABLE V

Typical Parametric Representations Proposed for Austenitic Stainless Steels

Equation	Reference
$\sigma = K_1 \epsilon^{n_1} + \exp K_2 \exp n_2 \epsilon$	[12]
K_1, n_1, K_2, n_2 are constants	
$\sigma = (\sigma_o - \sigma_\infty)\exp(-\epsilon/\epsilon_c) + \sigma_\infty$	[13]
σ_o, σ_∞, ϵ_c are constants	
$\sigma - \sigma_p = \frac{CP\epsilon}{1 + P\epsilon} + \hat{H}\epsilon_p$	[4]
C, $\hat{H}$, P are constants	
$\epsilon_L = \frac{\sigma}{E} + \left[\frac{\sigma - \sigma_p}{K}\right]^{1/m}$	[14]
K, m are constants	

See Appendix C for the definition of all other symbols.

at fracture. Furthermore, phenomena such as strain-aging or martensite formation are not presently amenable to analysis.

Uranium

The choice of uranium or dilute uranium alloys for nuclear shielding applications is principally predicated on their high density (18.9 gm/cm^3) and atomic number. Some authors [15] suggest that these materials may be considered structurally equivalent to mild steel. However, this assumption is generally unfounded and is extremely misleading.

Pure uranium undergoes three phase changes between -40°C and its melting point. Between -40 and 633°C, the temperature region of primary interest in this examination, its crystal structure is orthorhombic. Between 663 and 700°C it has a complex tetragonal structure, and above 770°C it undergoes a transition to body centered cubic.

The orthorhombic crystal structure of the alpha (or low temperature) phase suggests that the mechanical and physical properties of uranium will be highly anisotropic. For example, Appendix A shows that the thermal expansion behavior of single crystal α-uranium, may vary by a factor of 5, depending upon the particular crystallographic direction being considered. Practically, this large anisotropy in thermal expansion results in some grains being stressed beyond yield upon cooling. Subsequent application of a load will then result in plastic flow at vanishingly small stresses [16,17].

Another complication which arises because of the anisotropic nature of α-uranium is that both its elastic and plastic properties (e.g., strain hardening behavior) are dependent upon prior processing history. Highly textured material, where nearly all of the elastically "strong" directions are aligned, shows a twofold difference in elastic modulus between the "strong" and "weak" directions (see Appendix B). Few previous investigators have measured or even considered this textural effect when discussing the plastic deformation of uranium. This fact makes direct comparisons between various studies difficult and may explain some of the scatter observed.

The mechanical properties of depleted α-uranium are also quite sensitive to temperature (Figure 13). Decreasing the test temperature from 663°C results in an increase in tensile yield and ultimate strength. This increase is accompanied (to approximately 350°C) by a decrease in tensile ductility. Between 350 and 25°C the ductility appears to be essentially independent of temperature, or may exhibit a slight minima. Finally, below 25°C the ductility decreases sharply (i.e., α-uranium undergoes a ductile-brittle transition at about 25°C). These ductility changes have been associated with fracture transitions from ductile failure, involving inclusions [18,19], to mixed ductile plus intergranular failure and, finally, to twin-matrix [19] cleavage failure at the lowest test temperature.

The ranges over which the differing temperature-ductility relationships are observed can be altered in addition by changing test conditions, α-uranium microstructure, chemistry, etc. The

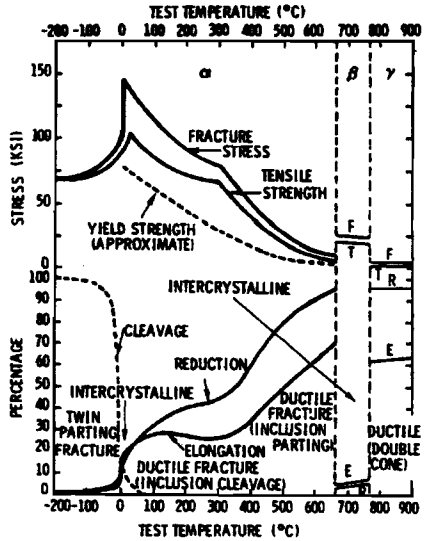

Figure 13. The effect of test temperature (-200°C to +900°C) on the tensile properties and fracture of uranium [18].

ductile-brittle transition temperature has been found to increase with increasing strain rate [21,22], grain size [17,18], grain shape irregularity [23,24], internal hydrogen content [22, 25-29], iron and aluminum content [24], residual stress level [30], humidity [31-33], and decreasing amounts of prior strain [17,34, 35]. The effect of one of these variables, grain size, on the transition temperature is shown in Figure 14. A quantitative assessment of the other variables awaits more detailed experimental studies.

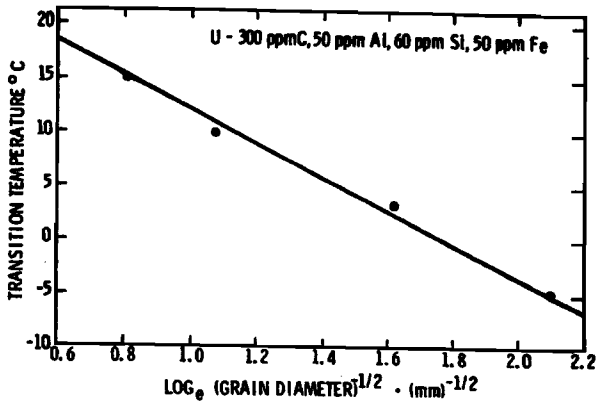

Figure 14. Ductile/brittle transition temperature versus $\log_e$ (grain diameter)$^{-1/2}$ for U - 300 ppm C, 50 ppm Al, 60 ppm Si, and 50 ppm Fe [3].

In a similar fashion, the ductility above the ductile-brittle transition region may be decreased by decreasing purity [36] and increasing residual stress [36,37]. Differences in residual stress level may also affect the strain hardening behavior of α-uranium. Figure 15(a) shows a family of serrated load-elongation curves of α-uranium in which the samples have had a high residual stress level induced in them by quenching from elevated temperature. If the same material had been furnace cooled, serrated yielding behavior would not have been observed (Figure 15(b)). The residual stress levels associated with these two heat treatment procedures were not reported so that our understanding of the influence of residual stress on the

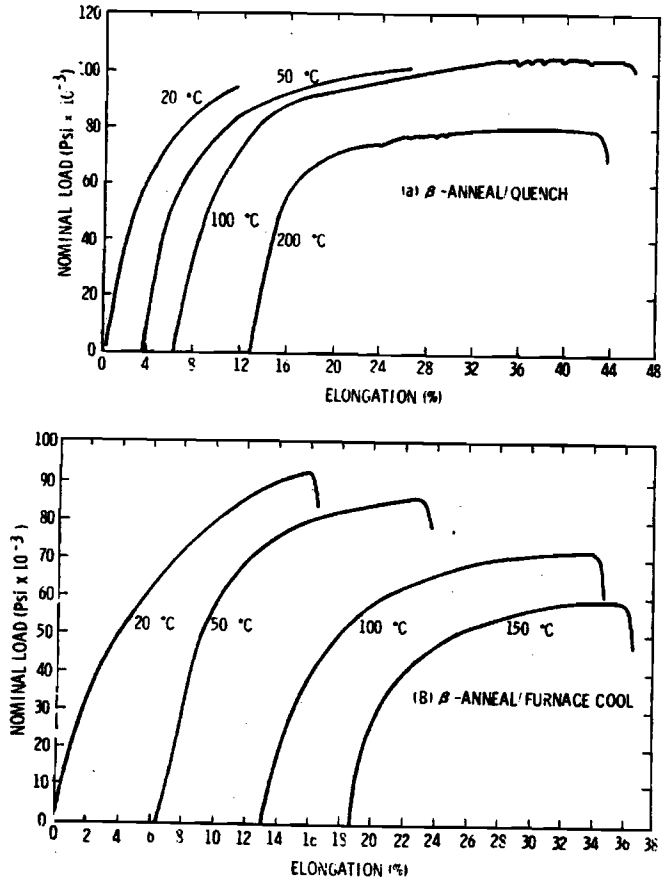

Figure 15. Load-elongation curves of α-uranium (U - 140 ppm C, 30 ppm Al, 140 ppm Fe, 60 ppm Si, 40 ppm O_2). Strain rate 2.6 x 10^{-4} sec^{-1} [37].

tensile ductility in the temperature region 50 to 350°C remains qualitative. The same situation exists with regard to the impurity effects since no quantitative examination has been reported.

Finally, Figures 16 and 17 represent a summary of the presently available stress-strain curves for α-uranium. It should be recognized that neither of these series is for as-cast α-uranium; to date attempts to locate same have been unsuccessful. Notwithstanding this, it appears that the changes in strain hardening behavior that would be anticipated by increasing strain

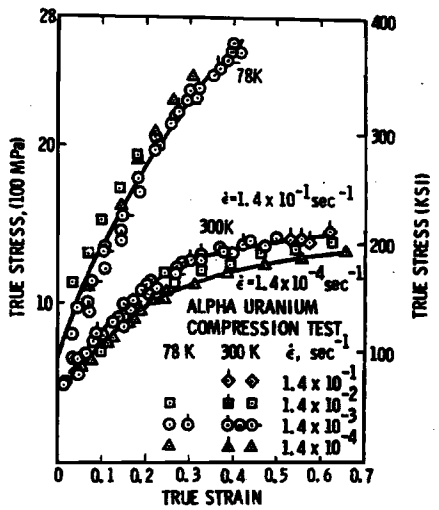

Figure 16. Influence of strain rate on the true-stress versus true-strain curves of annealed polycrystalline α-uranium (110 ppm C, 35 ppm Al, 70 ppm Si, 15 ppm Cr, 8 ppm Mo, 60 ppm Fe, 40 ppm Ni, 6 ppm Cu) at 78 and 300 K (-195 and 27°C)[38].

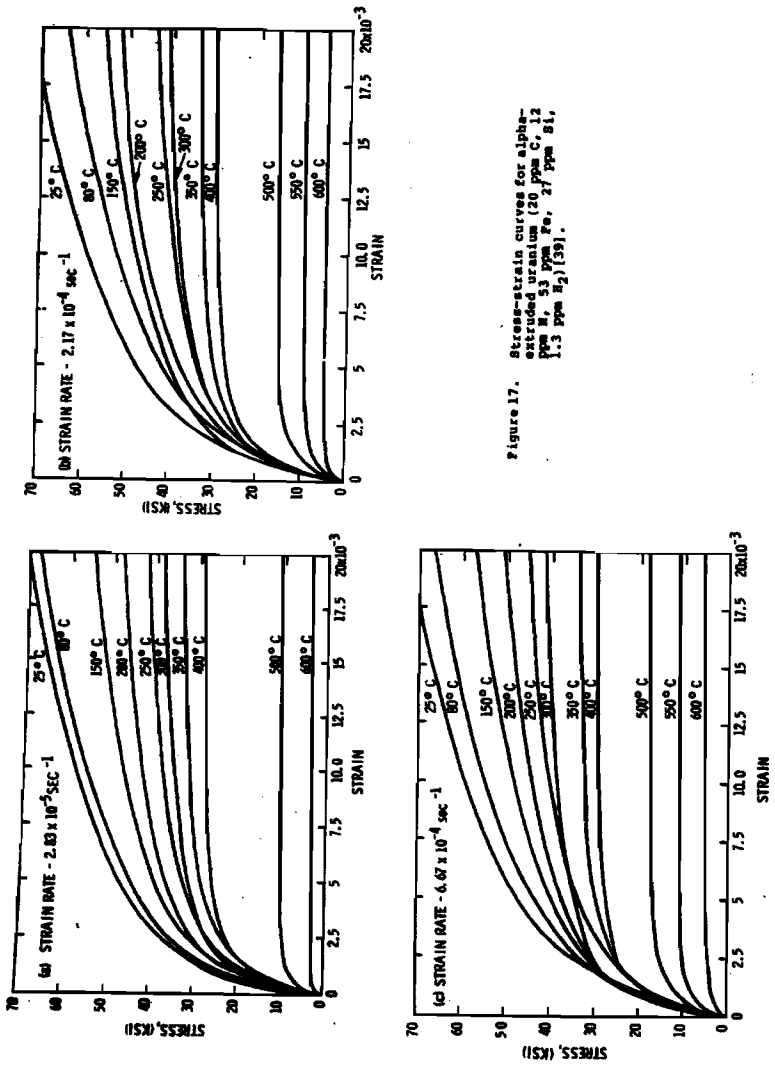

Figure 17. Stress-strain curves for alpha-extruded uranium (20 ppm C, 12 ppm N, 53 ppm Fe, 27 ppm Si, 1.3 ppm H_2)[39].

rate appear quite small and that the changes in flow stress and strain hardening behavior with changing temperature appear to be of paramount importance.

These results all suggest that depleted α-uranium should not at present be considered as a primary structural member since it undergoes a sharp loss in ductility with decreasing temperature. However, there is some evidence which suggests that appropriately heat treated uranium alloys (e.g., U-2 wt% Mo) may have a ductile-brittle transition temperature well below that of α-uranium (compare Figures 13 and 18).

Lead

A review of those physical, chemical, and mechanical characteristics of lead which have resulted in its widespread use for nuclear shielding has been given by Stukenbroeker et al. [40]. Paramount among these is lead's high density (ρ_{293K} = 11.35 gm/cm^3), low cost, and relative ease of fabrication. Although the present examination is limited to "chemical" lead, various other lead purities and alloys may be selected for nuclear applications.

The terminology "chemical" lead is generally restricted to material as specified by ASTM B29-55. Table I shows the standard chemical specification for this grade of pig lead, silver and copper being the principal impurities. Consideration of the Pb-Ag and Pb-Cu binary phase diagrams (Figure 19) suggests that while the Ag impurity concentration lies within the expected range of solid solubility, the presence of 0.04 to 0.08 weight percent copper will result in the formation of a two-phase

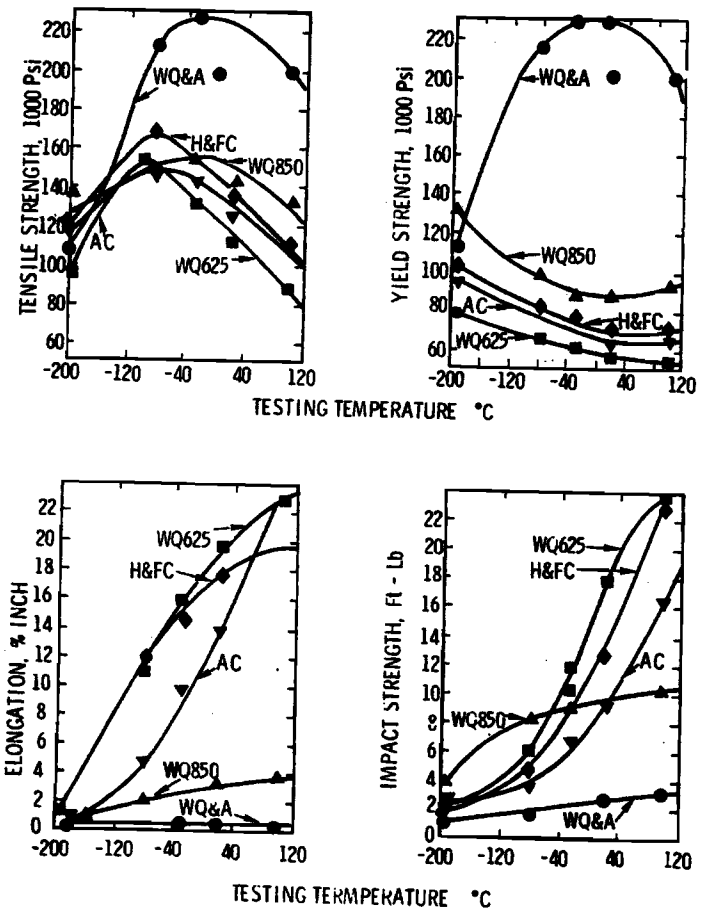

Figure 18. Mechanical properties of uranium-2 weight percent Mo (WQ&A: Water Quench and AGe; H&FC: Homogenize and Furnace Cool; AC: Air Cool)[20].

rate appear quite small and that the changes in flow stress and strain hardening behavior with changing temperature appear to be of paramount importance.

These results all suggest that depleted α-uranium should not at present be considered as a primary structural member since it undergoes a sharp loss in ductility with decreasing temperature. However, there is some evidence which suggests that appropriately heat treated uranium alloys (e.g., U-2 wt% Mo) may have a ductile-brittle transition temperature well below that of α-uranium (compare Figures 13 and 18).

Lead

A review of those physical, chemical, and mechanical characteristics of lead which have resulted in its widespread use for nuclear shielding has been given by Stukenbroeker et al. [40]. Paramount among these is lead's high density (ρ_{293K} = 11.35 gm/cm^3), low cost, and relative ease of fabrication. Although the present examination is limited to "chemical" lead, various other lead purities and alloys may be selected for nuclear applications.

The terminology "chemical" lead is generally restricted to material as specified by ASTM B29-55. Table I shows the standard chemical specification for this grade of pig lead, silver and copper being the principal impurities. Consideration of the Ag-Pb and Pb-Cu binary phase diagrams (Figure 19) suggests that the Ag impurity concentration lies within the expected range of solid solubility, the presence of 0.04 to 0.08 weight percent copper will result in the formation of a two-phase

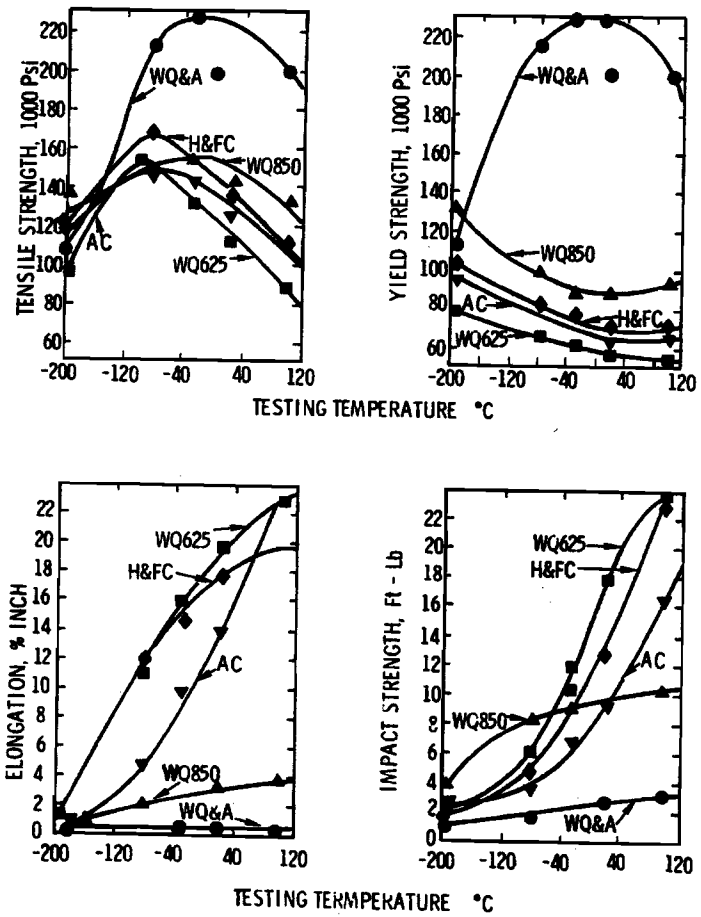

Figure 18. Mechanical properties of uranium-2 weight percent Mo (WQ&A: Water Quench and AGe; H&FC: Homogenize and Furnace Cool; AC: Air Cool)[20].

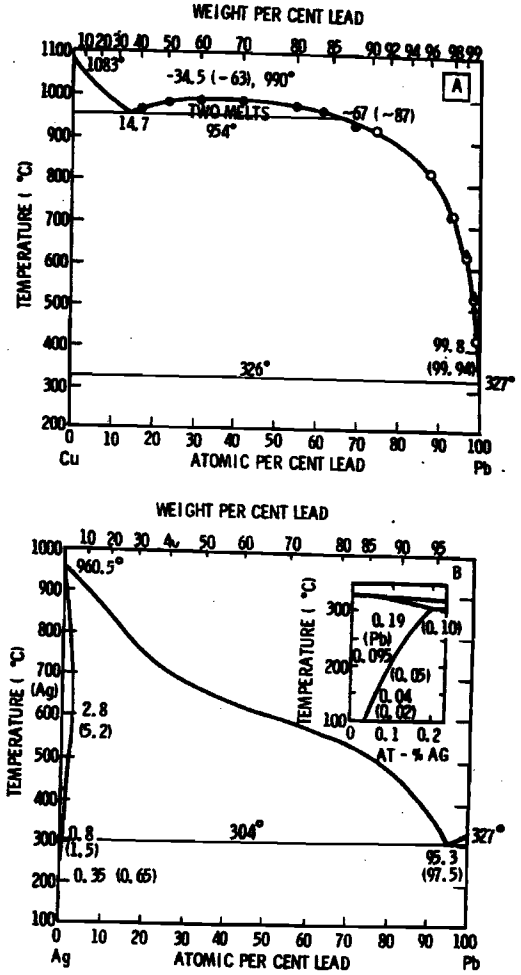

Figure 19. Phase diagrams for (a) copper-lead and (b) silver-lead [41].

(Cu+Pb) alloy. It is, therefore, not surprising that this small amount of copper has been reported to have a noticeable effect on the mechanical properties of lead.

Although there have been a number of examinations of the influence of strain-rate and temperature on the mechanical behavior of lead [42,56], application of these data to shipping cask environments is not straightforward. In general, the available data do not include a description of either the chemistry or thermomechanical condition for the material being examined. Under these circumstances probably the most complete series of experiments that have been performed to date are those of Tietz [51] (Figure 20 through 23) and Green et al. [56] (Figures 24 and 25). The former author's results demonstrate that the mechanical behavior of lead is quite sensitive to chemistry. Indeed, at low temperatures high purity (99.995 percent) lead is stronger than lead containing 0.058 weight percent Cu, contrary to what might be expected while at temperatures above 373 K (100°C), the opposite trend is observed (Figure 26). It is also interesting to note that the more recent results of Evans [45] (Figures 27 and 28) do not agree with those of Tietz. Presently, the cause of this discrepancy is undefinable, since Evans simply reported his material as "chemical" lead without giving any information as to the actual chemistry, grain structure, etc.

One final comment must be made regarding mechanical property reproducibility at high-strain rates. Generally the observed measurement errors are large and, more importantly, are unpredictable. For example, the undulations observed in the

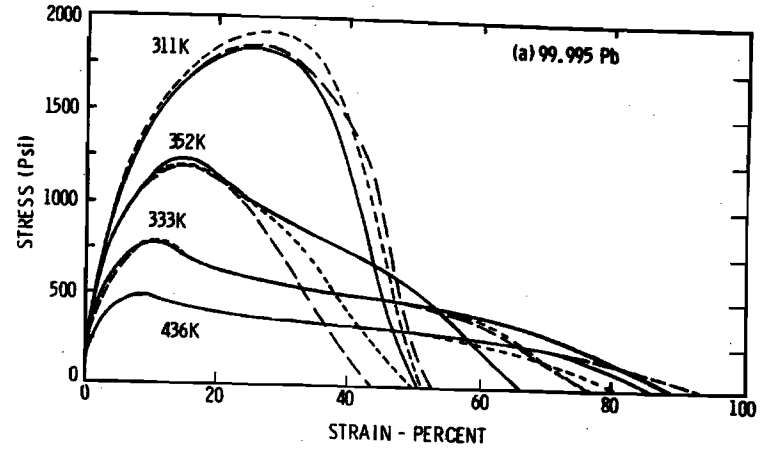

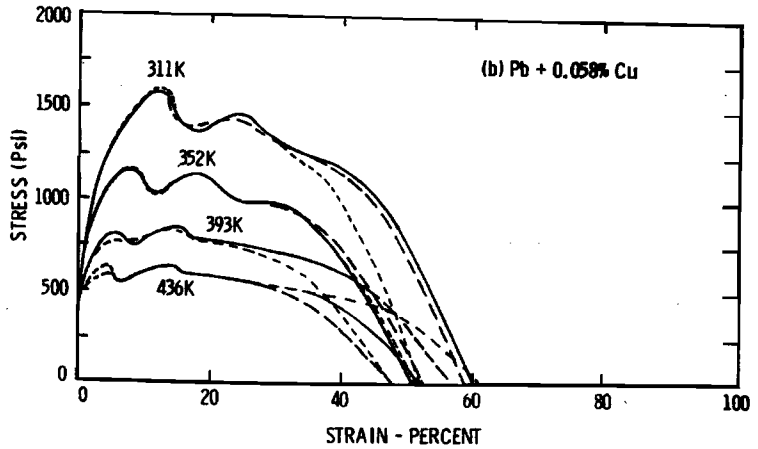

Figure 20. Triplicate tensile stress-strain curves to failure at a strain rate of 1 x 10^{-3} sec^{-1} [51].

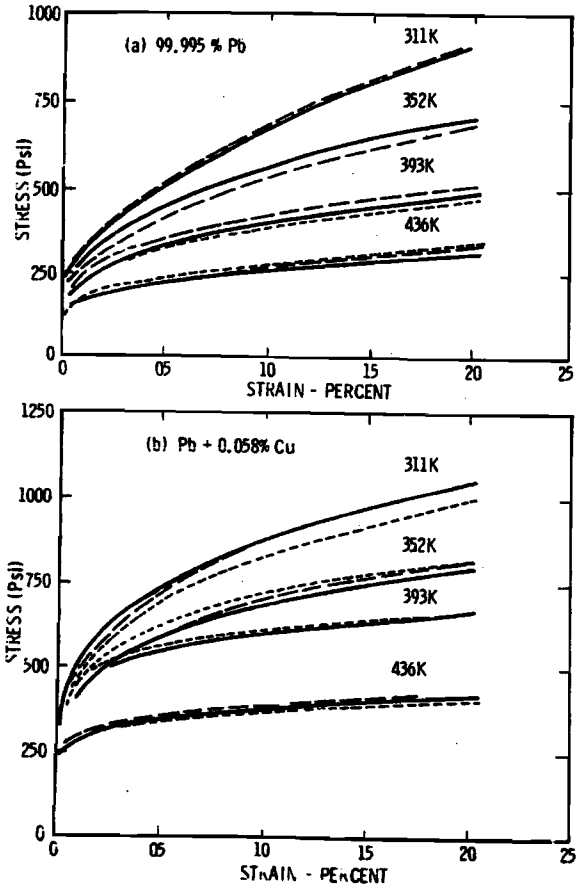

Figure 21. Triplicate tensile stress-strain curves to 2 percent strain at a strain rate of 8.3 x 10^{-5} sec^{-1} [51].

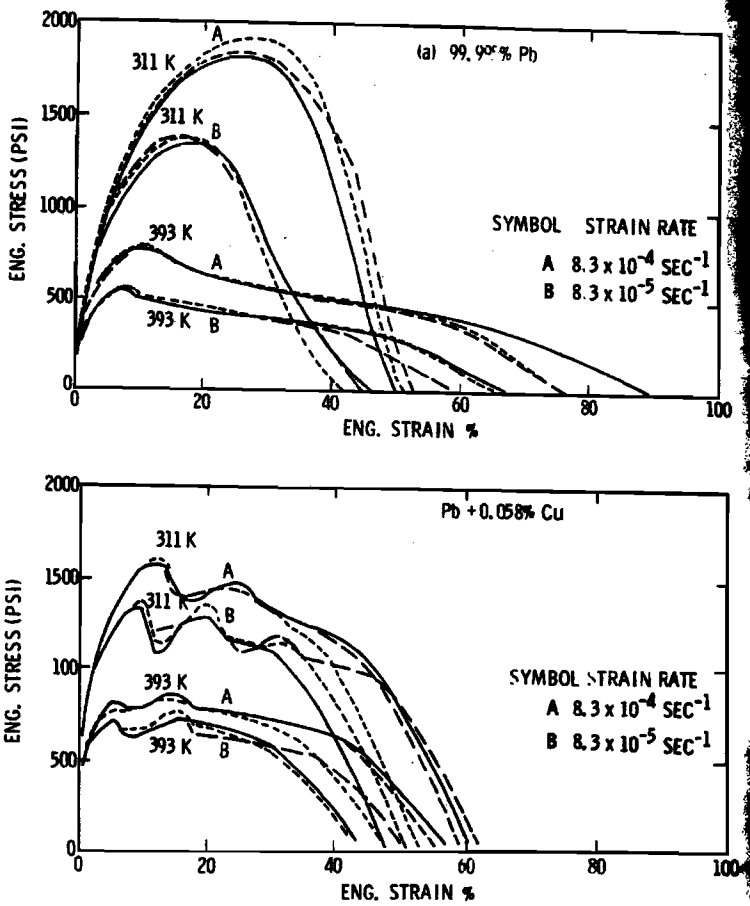

Figure 22. Effect of strain rate on the tensile stress-strain curves at 311 and 393 K (triplicate curves) [51].

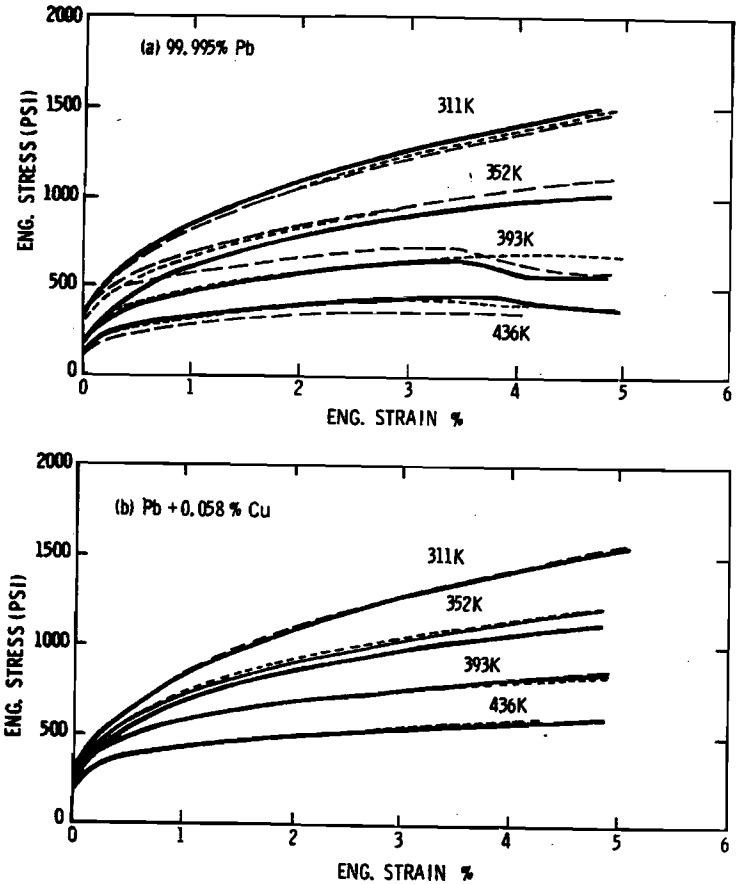

Figure 23. Triplicate compression stress-strain curves to 5 percent strain at a strain rate of 2.5 x 10^{-4} sec^{-1} [51].

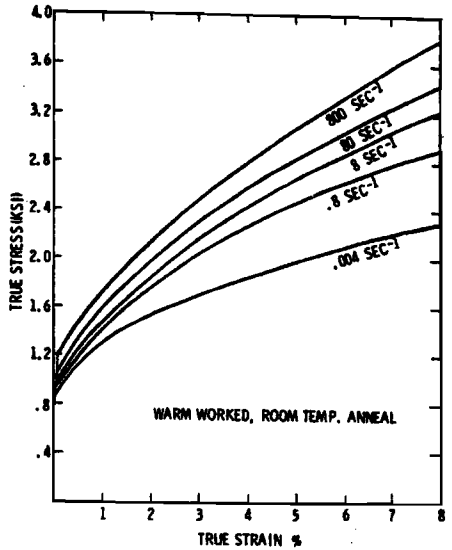

Figure 24. Stress-strain curves for Pb [56].

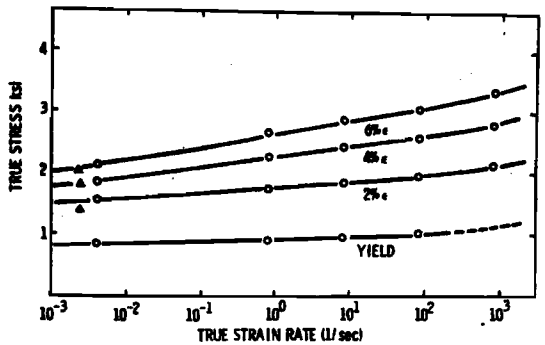

Figure 25. Influence of strain rate on flow stress of Pb [56].

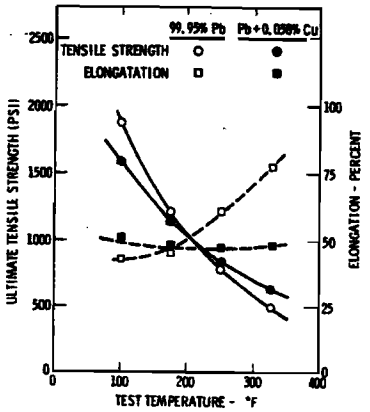

Figure 26. Tensile strength and elongation as a function of test temperature at a strain rate of 8.3×10^{-4} sec^{-1} [51].

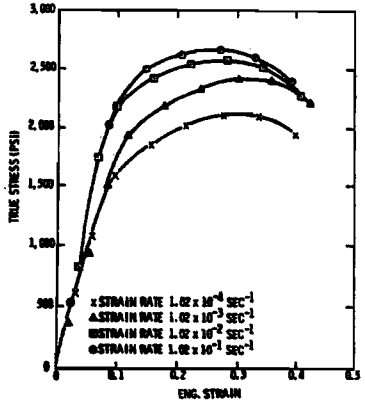

Figure 27. Quasi-static true stress-strain curves for chemical lead test specimens in tension [45].

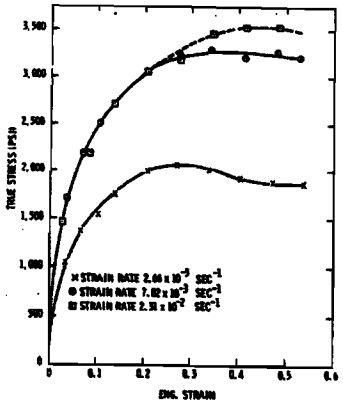

Figure 28. Quasi-static true stress-strain curves for chemical lead test specimens in compression [45].

stress-strain curves shown in Figure 29 bear little relationship to each other even though they are reported to be results of tests ostensibly carried out at different strain rates on the same lot of material. It is clear that much more care will have to be exercised in any further examination of the mechanical behavior of lead and its alloys.

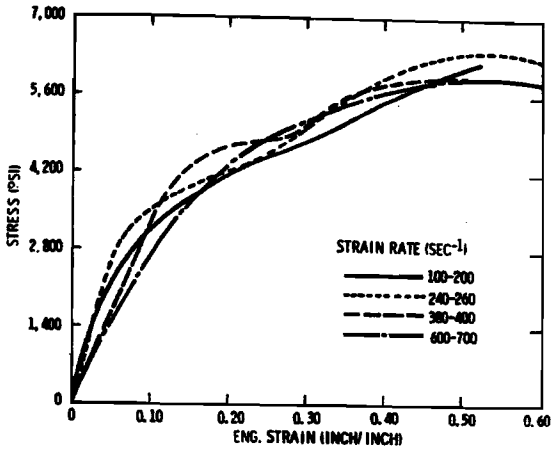

Figure 29. Stress-strain curves of lead for four strain-rate ranges [45].

Summary and Recommendations

This review of the available literature has shown that there are many areas which require further attention before an adequate data base will be established for use with increasingly sophisticated finite-element computer programs. Listed below are the

authors' recommendations of those subjects which will require further evaluation.

Mechanical Properties

1. Define the temperature, strain-rate, and strain regions for which strain-induced martensite and dynamic strain-aging will control the stress-strain behavior of the austenitic stainless steels used for LWR shipping casks.

2. Establish a data base for selected austenitic stainless steels, "chemical" lead, and as-cast α-uranium. The data base should include:

   a. The influence of strain-rate and temperature on the tensile, compressive, and shear properties.
   b. The influence of chemistry variation on the mechanical properties.
   c. The influence of residual stress level and test environment on the mechanical behavior of as-cast α-uranium.

3. Develop constitutive equations to describe the stress-strain behavior of LWR shipping cask material under both normal and abnormal (due to strain aging or martensitc formation) modes of deformation.

Thermal Expansion (See Appendix A)

1. Establish the thermal expansion behavior of 216, 317, 321, and 347 stainless steel over the temperature range -40 to 320°C (-40 to 620°F).

2. Establish the thermal expansion behavior of typical product forms of α-uranium used in shipping cask applications. Particular attention should be given to the expected anisotropic orientation dependence of the thermal expansivity.

Elastic Properties (See Appendix B)

1. Extend moduli measurements for austenitic steels (304, 316, 321, 347) to the lowest operating temperatures (-40°C) associated with shipping casks.

2. Determine elastic properties of 216, 308, 317, and 347 stainless steel.

3. Determine elastic properties of selected dilute uranium alloys (e.g., U-2Mo).

The primary emphasis of all of these studies should be a systematic and quantitative assessment including pertinent microstructural information rather than the largely qualitative information available at the present time.

References

Stainless Steels

1. Aerospace Structural Metals Handbook, Vol. 2, AFML-TR-68-115, Mechanical Properties Data Center, Belfour Stulen, Inc. (1975).

2. G. P. Sanderson and D. T. Llewellyn, "Mechanical Properties of Standard Stainless Steels in the Temperature Range -196°C to +800°C," J. Iron Steel Inst. 207, 1129 (1969).

3. H. E. McCoy, Jr., and R. D. Waddell, "Mechanical Properties of Several Products from a Single Heat of Type 304 Stainless Steel," J. Eng. Mat. Tech. 97, 343 (1975).

4. J. P. Hammond and V. K. Sikka, Heat-to-Heat Variations of Total Strain (to 5%) at Discrete Stress Levels in Types 316 and 304 Stainless Steel from 24° to 316°C, ORNL/NUREG-TM-57, Oak Ridge National Laboratory, Oak Ridge, TN (November 1976).

5. A. Rosen R. Jago, and T. Kjer, "Tensile Properties of Metastable Stainless Steels," J. Matl. Sci. 7, 871 (1972).

6. C. F. Jenkins and G. V. Smith, "Serrated Plastic Flow in Austenitic Stainless Steel," Trans. AIME 245, 2149 (1969).

7. J. T. Barnby, "Effect of Strain Aging on the High Temperature Tensile Properties of an AISI 316 Austenitic Stinless Steel," JISI 203 392 (1965).

8. H. Yamada and Li Che-yu, "Stress-Relaxation and Mechanical Equation of State in Austenitic Stainless Steels," Met. Trans. 4, 2133 (1973).

9. R. W. Rohde and J. C. Swearengen, "A Mechanical Equation of State for Inelastic Deformation of Iron: An Analytic Description," J. Eng. Matls. Tech. 99, 59 (1977).

10. R. W. Swindeman, "Representation of the High-Temperature Tensile Behavior of Re-Annealed Type 304 Stainless Steel by the Voce Equation," J. Eng. Matls. Tech. 97H, 98 (1975).

11. J. M. Steichen, "Mathematical Description of the Elevated Temperature Flow Behavior of Type 304 Stainless Steel at High Strain Rates," J. Test. Eval. 1, 520 (1973).

12. D. C. Ludwigson, "Modified Stress-Strain Relation for FCC Metals and Alloys," Met. Trans. 2, 2825 (1971).

13. E. Voce, "The Relationship Between Stress and Strain for Homogeneous Deformation," J. Inst. Metals 74, 537 (1948).

14. Nuclear Systems Materials Handbook, Vol. 1, TID 26666, Hanford Engineering Development Laboratory, Richland, WA (1975).

Uranium

15. E. B. Blasch, G. Stukenbroeker, R. J. Lusky, C. Bonilla, and H. Berger, "The Use of Uranium as a Shielding Material," Nucl. Engr. & Design 13, 146 (1970).

16. D. Calais, G. Saada, and N. Simenel, "Influence of the Anisotropy of the Expansion Coefficient on the Elastic Properties of Uranium, Zirconium, and Zinc," Comptes Rendus 249, 1225 (1959)

17. D. M. R. Taplan and J. W. Martin, "The Effect of Grain Size and Cold Work on the Tensile Properties of Alpha Uranium," J. Less Common Metals 7, 89 (1964).

18. D. M. R. Taplin, "The Tensile Properties and Fracture of Uranium Between -200°C and 900°C," Australian Inst. Met. J. 12, 32 (1967).

19. D. M. R. Taplin and J. W. Martin, "The Metallography and Fracture of Alpha Uranium," Metallurgia 71, 83 (1965).

20. E. G. Sukas, "Properties of As-Cast and Heat Treated 2% Molybdenum-Uranium," Trans. ASM 51, 752 (1959).

21. F. Jean-Louis and P. Lacombe, "Plastic Deformation of Polycrystalline Uranium Under Tension at Various Strain Rates Between 20 and 850°C," Compt. Rend. Ser. C. 262, 316 (1966).

22. P. D. Tilburg, Impact Testing of Uranium, AWRE O-33/66, (March 1966).

23. D. M. R. Taplin and J. W. Martin, "The Effect of Grain Shape on the Tensile Properties of -Uranium," J. Nucl. Matls. 10, 134 (1963).

24. D. M. R. Taplin and J. W. Martin, "The Effect of Small Additions of Iron and Aluminum on the Tensile Properties of Alpha Uranium," J. Nucl. Matls. 12, 50 (1964).

25. W. L. Owen, "Effect of Hydrogen on Mechanical Properties of Uranium," Metallurgia 66, 3 (July 1962).

26. C. Prunier, M. Linard, and F. Giraud-Heraud, "Influence de L'hydrogen Internal sur les Proprietes Mecaniques et Structurales de L'alliage Uranium - 0.2% pds Vanadium," J. Nucl. Matls. 64, 14 (1977).

27. A. N. Hughes, S. Orman, and G. Picton, "Some Effects of Hydrogen in Uranium," Proc. Intl. Conf. on Hydrogen in Metals, Paris (1972) p. 466.

28. H. R. Gardner and J. W. Riches, "The Effect of Uranium Hydride Distribution and Recrystallization on the Tensile Properties of Uranium," Trans. ASM 52, 728 (1960).

29. G. L. Powell and J. B. Condon, "Hydrogen in Uranium Alloys," in Physical Metallurgy of Uranium Alloys, J. J. Burke, D. A. Colling, A. E. Gorum, and J. Greenspan, eds., Brook Hill Publishing Company, Chestnut Hill, MA (1976) p. 427.

30. D. M. R. Taplin and J. W. Martin, "An Effect of Thermal Cycling Upon the Ductility Transition in Alpha Uranium," J. Inst. Metals 93, 230 (1964).

31. A. N. Hughes, S. Orman, and G. Picton, "Environmental Factors Affecting the Mechanical Properties of Uranium, Part I - The Effect of Water Vapour," J. Nucl. Matls. 33, 159 (1969).

32. A. N. Hughes, S. Orman, and G. Picton, "Environmental Factors Affecting the Mechanical Properties of Uranium, Part II - The Mechanism of the Water Embrittlement of Uranium," J. Nucl. Matls. 33, 165 (1969).

33. A. N. Hughes, S. Orman, G. Picton, and M. A. Thorne, "The Effect of Humidity on the Low Temperature Tensile Properties of Uranium," J. Nucl. Matls. 33, 99 (1969).

34. P. D. Tilbury, Experiments to Improve the Mechanical Properties of Wrought Uranium, AWRE 038/68, (June 1968).

35. J. Bolton and P. D. Tilbury, "The Influence of Warm Rolling Upon the Ductile/Brittle Transition Temperature ofα-Uranium," J. Inst. Metals 92, 95 (1963-64).

36. A. Lemogne and P. Lacombe, "Plastic Deformation in Uniaxial Tension of Monocrystals and Polycrystalline Uranium Between 20°C and 196°C," J. Nucl. Matls. 16, 129 (1965).

37. C. J. Beevers and G. T. Newman, "The Influence of Heat Treatment on the Tensile Behavior of Uranium in the Temperature Range 200-200°C," J. Less Common Metals 14, 225 (1968).

38. P. A. Loretan and G. Murphy, "The Influence of Rate of Loading and Temperature on the Tensile Properties of Normal Alpha Uranium," Proc. ASTM 64, 734 (1964).

39. J. E. Hockett, P. S. Gilman, and O. D. Sherby, "Compressive Deformation of Polycrystalline Uranium at Low Temperatures," J. Nucl. Matls. 64, 231 (1977).

Lead

40. G. L. Stukenbroeker, C. F. Bonilla, and R. W Peterson, "The Use of Lead as a Shielding Material," Nucl. Engr. & Design 13, 3 (1970).

41. M. Hansen, Constitution of Binary Alloys, 2nd Edition, McGraw-Hill, New York (1958).

42. U. S. Lindholm, "Some Experiments with the Split Hopkinson Pressure Bar," J. Mech. Phys. Solids 12, 317 (1964).

43. J. M. Gondusky and J. Duffy, The Dynamic Stress-Strain Relation of Lead and Its Dependence on Grain Structure, Tech. Rpt. No. 53, Brown University, Providence, RI (May 1967).

44. C. H. Mok and J. Duffy, "The Dynamic Stress-Strain Relation of Metals as Determined from Impact Tests with a Hard Ball," Intl. J. Mech. Sci. 7, 355 (1965).

45. J. H. Evans, Structural Analysis of Shipping Casks, Vol. 8, Experimental Study of the Stress-Strain Properties of Lead Under Specified Impact Conditions, ORNL-TM-1312, Oak Ridge National Laboratory, Oak Ridge, TN (August 1970).

46. L. D. Skolov, "A Systemmatic Study of the Dependence of Speed and Temperature of the Resistance to Deformation in One-Phase Metals," Dokl. Akad, Nauk SSSR 70, 839 (1950).

47. H. E. Cline and T. H. Alden, "Rate-Sensitive Deformation in Tin-Lead Alloys," Trans. AIME 239, 710 (1967).

48. J. A. Bailey and A. R. E. Singer, "Effect of Strain Rate and Temperature on the Resistance to Deformation of Aluminum, Two Aluminum Alloys, and Lead," J. Inst. Metals 92, 404 (1963-64).

49. L. D. Skolov, "The Effect of Temperature and Strain Velocity of the Resistance to Deformation of Metals," Russian Met. and Mining 3, 93 (1963).

50. N. Lorzon and R. B. Sims, "The Yield Stress of Pure Lead in Compression," J. Mech. Phys. Solids 1, 234 (1953).

51. T. E. Tietz, "Mechanical Properties of a High-Purity Lead and a 0.058 Percent Copper-Lead Alloy at Elevated Temperatures," Proc. ASTM 59, 1052 (1959).

52. F. A. Hodierne, "A Torsion Test for Use in Metal Working Studies," J. Inst. Metals 91, 267 (1962-63).

53. H. Kolsky, "An Investigation of the Mechanical Properties of Materials at Very High Rates of Loading," Proc. Phys. Soc. 62B, 676 (1949).

54. E. R. Parker and C. Ferguson, "The Effect of Strain Rate Upon Tensile Impact Strength of Some Metals," Trans. ASM 30, 68 (1942).

55. R. F. Steidel and C. F. Makesov, "The Tensile Properties of Some Engineering Materials at Moderate Rates of Strain," ASTM Bulletin No. 247, 57 (1960).

56. S. J. Green, C. J. Maiden, S. G. Babcock, and F. L. Schierloh, The High Strain-Rate Behavior of Face Centered Cubic Metals," MSL-69-36, GM Technical Center, (October 1969).

Thermal Expansion

57. Y. S. Touloukian, R. K. Kirby, R. E. Taylor, and P. D. Desai, Thermophysical Properties of Matter, Vol. 12, Plenum Press, New York (1975).

58. D. E. Furman, "Thermal Expansion Characteristics of Stainless Steels Between -300 and 1000°F," Trans. AIME 188, 688 (1950).

59. R. D. Seibel and G. L. Mason, Thermal Properties of High Temperature Materials, WADC-TR-57-468, U.S. Air Force (1958).

Elastic Properties

60. Source Book on Stainless Steels, American Society for Metals, Metals Park, OH (1976) p. 95.

61. A. J. Goldman and W. D. Robertson, "Elastic Properties of Austenite and Martensite in Iron-Nickel Alloys," Acta Met. 12, 1265 (1964).

62. O. D. Sherby, D. L. Bly, and D. H. Wood, "Plastic Flow and Strength of Uranium and Its Alloys," in Physical Metallurgy of Uranium Alloys, J. J. Burke, D. A. Colling, A. E. Gorum, and J. Greenspan, eds., Brook Hill Publishing Company, Chestnut Hill, MA (1976) p. 311.

63. E. S. Fisher, "Temperature Dependence of the Elastic Moduli in Alpha Uranium Single Crystals, Part IV (298 to 932 K)," J. Nucl. Matls. 18, 39 (1966).

64. P. E. Armstrong, D. T. Eash, and J. E. Hockett, "Elastic Moduli of Alpha, Beta, and Gamma Polycrystalline Uranium," J. Nucl. Matls. 45, 211 (1972-73).

65. W. Koster, "Die Temperaturabhagegkeit des Elastizitats-moduls reiner Metalle," Zeit. fur Metkde 39, 1 (1948).

APPENDIX A

Thermal Expansion Behavior of Selected Stainless Steels, Uranium, and Lead

The thermal expansion behavior of stainless steel, uranium, and lead are presented below. The linear thermal expansion has been presented as $\Delta L/L_o$ where (see Appendix C for definition of symbols):

$$\Delta L = L_T - L_o$$

Stainless Steels

The thermal expansion behavior of the stainless steels presently being considered is tabulated in Table A-I and summarized in Figure A-1. The data are quite limited; none were found for 216 or 317 stainless steels. In addition, that for 321 stainless is well above the temperature range of primary interest for shipping applications. However, Figure A-1 does suggest that the thermal expansivity of many stainless steels is quite similar and that, to a first approximation, they may be represented by that of 304 stainless steel, i.e. [57],

$$\Delta L/L_o(\%) = 0.358 + 9.471 \times 10^{-4}\, T + 1.031 \times 10^{-6} T^2 - 2.978 \times 10^{-10} T^3 \quad (T \text{ in } °K)$$

The formation of martensite at low temperature or δ-ferrite in weldments can be expected to alter this behavior in an as yet undetermined manner.

TABLE A-I

Thermal Linear Expansion of Stainless Steel
304 Stainless (19.19 Cr, 8.49 Ni, 0.65 Mn, 0.53 Si,
0.068 C, 0.024 P, 0.007 S, balance Fe)[58]

Temperature (K)	L/L_o(%)	Temperature (K)	L/L_o(%)
233	-0.089	405	0.182
239	-0.083	411	0.191
244	-0.076	416	0.199
250	-0.071	422	0.207
255	-0.058	436	0.236
261	-0.046	450	0.259
266	-0.040	464	0.281
272	-0.029	478	0.309
278	-0.024	491	0.334
283	-0.013	505	0.358
289	-0.005	519	0.383
294	0.002	533	0.402
300	0.012	547	0.429
305	0.028	561	0.455
311	0.028	575	0.484
316	0.037	589	0.507
322	0.044	603	0.536
328	0.055	616	0.563
333	0.063	630	0.588
339	0.073	644	0.614
344	0.083	658	0.636
350	0.091	672	0.667
355	0.100	686	0.695
361	0.107	700	0.724
366	0.118	714	0.768
372	0.128	741	0.809
378	0.134	755	0.831
383	0.145	769	0.858
389	0.151	783	0.887
394	0.161	797	0.917
400	0.172	810	0.945

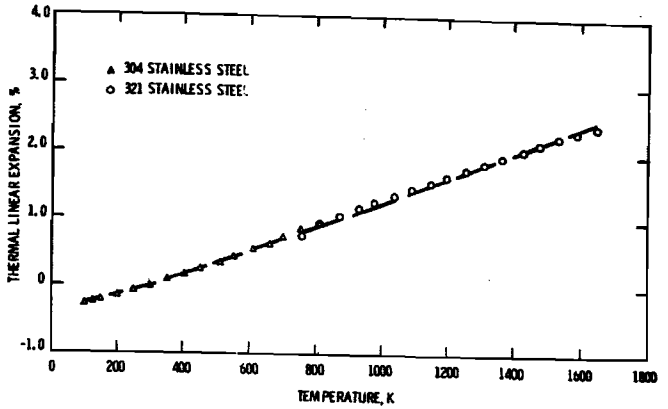

Figure A-1. Thermal expansion of 304 and 321 stainless steel.

Uranium

The thermal expansion behavior of α-uranium is quite complex (see Table A-II and Figure A-2). Single crystal measurements indicate that the expansion behavior, in contrast to stainless steel or lead, is highly anisotropic and depends upon the particular crystal-lographic orientation being considered. This suggests that the thermal expansion coefficients of polycrystalline uranium will be extremely sensitive to prior processing history and are expected to be quite variable. To date there have been no investigations of the influence of thermomechanical treatment on the thermal expansivity of α-uranium so that any formalism proposed to describe its behavior must be considered as only a first approximation.

TABLE A-II

Thermal Linear Expansion of Polystalline α-Uranium

Curve 13 (99.8 U, 0.14 C, 0.03 Si)		Curve 32 ("Pure" Uranium)	
Temperature (K)	$\Delta L/L_o$(%)	Temperature (K)	$\Delta L/L_o$(%)
291	-0.0032	293	0.000
373	0.127	373	0.118
473	0.306	473	0.268
573	0.506	575	0.424
673	0.728	673	0.594

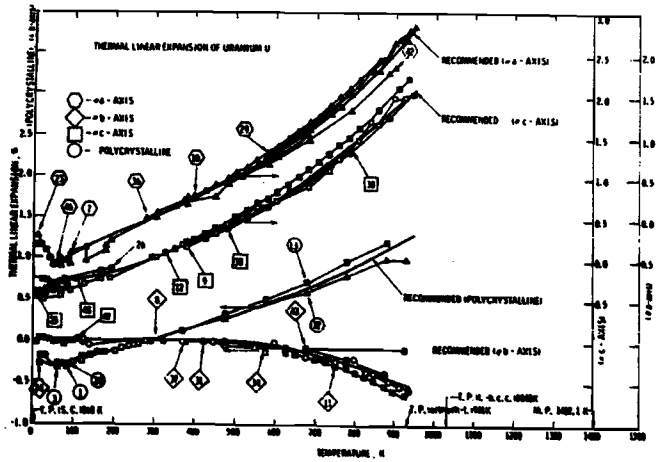

Figure A-2. Thermal expansion behavior of α-uranium, curve reference numbers given by Toulonkian et al. [57].

Notwithstanding, Touloukian et al. [57] recommend that the thermal expansion behavior of polycrystalline α-uranium can be represented by:

$$\Delta L/L_o(\%) = -0.379 + 1.264 \times 10^{-3}T - 8.982 \times 10^{-8}T^2 + 6.844 \times 10^{-10}T^3 \quad (293\ K < T < 941\ K).$$

(T in °K)

As noted above, the error limits to be associated with this relationship must be established.

Lead

The thermal expansion behavior of lead is summarized in Figure A-3. Although the bulk of this data refers to high purity lead it appears that, in those instances where the impurity levels approach that of "chemical" lead, the expansion behavior remains relatively unaffected. Indeed, it has been proposed that all of the tabulated values can be represented to within ± 3 percent over the temperature range 100 to 600 K by the following equation [57]:

$$\Delta L/L_o(\%) = 0.786 + 2572 \times 10^{-3}T + 1.147 \times 10^{-7}T^2 + 8.770 \times 10^{-10}T^3 \quad (T \text{ in } °K)$$

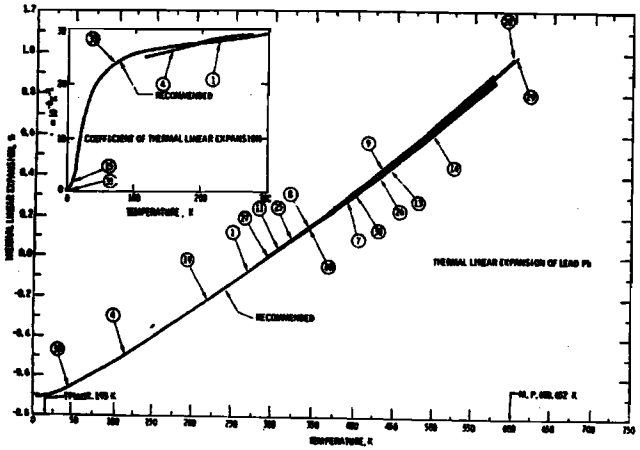

Figure A-3. Thermal expansion behavior of lead, curve reference numbers given by Touloukian et al. [57].

with the recommended values being

Temperature (K)	$\Delta L/L_o$ (%)	$\alpha \times 10^6 (K^{-1})$
100	-0.526	25.6
200	-0.261	27.5
293	0.000	28.9
400	0.317	30.6
500	0.638	33.3
600	0.988	36.7

where

$$\alpha = (1/L_{293})dL/dT$$

APPENDIX B

Elastic Properties of Selected Stainless Steels, Uranium, and Lead

Stainless Steels

Typical values for the elastic constants of selected stainless steels are given in Tables B-I through B-VII and Figures B-1 through B-6. Examination of this data indicates that variations in chemistry within the group of austenitic stainless steels presently under consideration have little effect on their elastic properties. Furthermore, increasing temperature generally results in a gradual decrease in the Young's and shear moduli and an accompanying increase in Poisson's ratio. Again, martensite formation can be expected to cause changes. For example, the presence of martensite has been shown to lower the modulus of the parent austenite phase [61].

TABLE B-I

Effect of Temperature on the Elastic Constants of Selected Stainless Steels [60]

Type	Temperature (K) 297	422	533	644
	Young's Modulus (10^3 ksi)			
304	29.0	27.3	26.0	24.8
316	28.4	27.2	26.4	25.6
317	27.0	26.4	25.0	-
321	28.9	27.3	25.8	24.5
347	28.9	27.5	26.1	24.8
	Shear Modulus (10^3 ksi)			
304	11.2	10.4	9.8	9.3
316	11.3	10.8	10.2	9.2
317	-	-	-	-
321	11.2	10.6	9.9	9.4
347	11.4	10.7	10.1	9.5
	Poisson's Ratio			
304	0.30	0.31	0.31	0.32
316	0.26	0.26	0.30	0.34
317	0.25	0.28	0.31	0.31
321	0.28	0.29	0.30	0.31
347	0.28	0.29	0.30	0.31

TABLE B-II

Young's Modulus for Annealed 304 Stainless Steel [14]

1971 ASME CODE

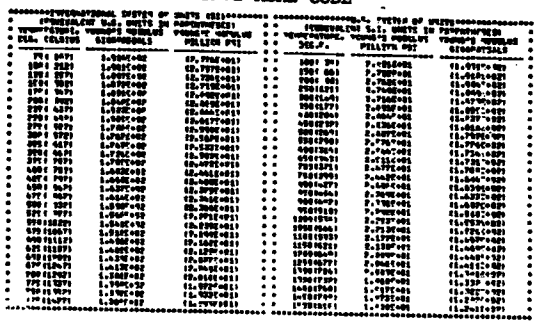

TABLE B-III

Shear Modulus for Annealed 304 Stainless Steel [14]

1971 ASME CODE

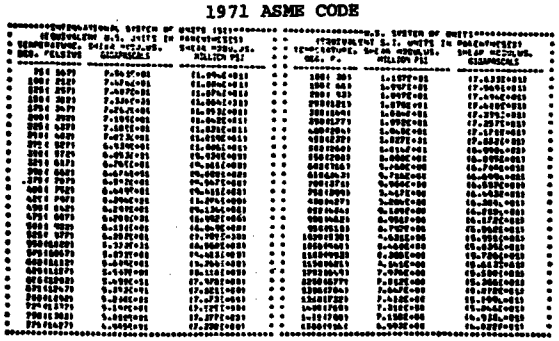

TABLE B-IV

Poisson's Ratio for Annealed 304 Stainless Steel [14]

INTERNATIONAL SYSTEM OF UNITS (SI) (EQUIVALENT U.S. UNITS IN PARENTHESES)		U.S. SYSTEM OF UNITS (EQUIVALENT S.I. UNITS IN PARENTHESES)	
TEMPERATURE, DEG. CELSIUS	POISSON'S RATIO	TEMPERATURE, DEG. F.	POISSON'S RATIO
75 (167)	2.894E-01	100 (38)	2.686E-01
100 (212)	2.717E-01	150 (66)	2.684E-01
125 (257)	2.741E-01	200 (93)	2.711E-01
150 (302)	2.762E-01	250 (121)	2.737E-01
175 (347)	2.784E-01	300 (149)	2.761E-01
200 (392)	2.634E-01	350 (177)	2.785E-01
225 (437)	2.824E-01	400 (204)	2.808E-01
250 (482)	2.844E-01	450 (232)	2.651E-01
275 (527)	2.862E-01	500 (266)	2.851E-01
300 (572)	2.881E-01	550 (288)	2.872E-01
325 (617)	2.899E-01	600 (316)	2.892E-01
350 (662)	2.917E-01	650 (343)	2.912E-01
375 (707)	2.934E-01	700 (371)	2.931E-01
400 (752)	2.951E-01	750 (399)	2.951E-01
425 (797)	2.969E-01	800 (427)	2.976E-01
450 (842)	2.966E-01	850 (454)	2.989E-01
475 (887)	3.003E-01	900 (482)	3.004E-01
500 (932)	3.022E-01	950 (510)	3.027E-01
525 (977)	3.037E-01	1000 (538)	3.046E-01
550 (1022)	3.055E-01	1050 (566)	3.066E-01
575 (1067)	3.072E-01	1100 (593)	3.086E-01
600 (1112)	3.091E-01	1150 (621)	3.106E-01
625 (1157)	3.110E-01	1200 (649)	3.127E-01
650 (1202)	3.122E-01	1250 (677)	3.140E-01
675 (1247)	3.147E-01	1300 (704)	3.171E-01
700 (1292)	3.167E-01	1350 (732)	3.194E-01
725 (1337)	3.184E-01	1400 (760)	3.217E-01
750 (1382)	3.219E-01	1450 (788)	3.242E-01
775 (1427)	3.211E-01	1500 (816)	3.266E-01

TABLE B-V

Young's Modulus for Annealed 316 Stainless Steel [14]

1971 ASME CODE

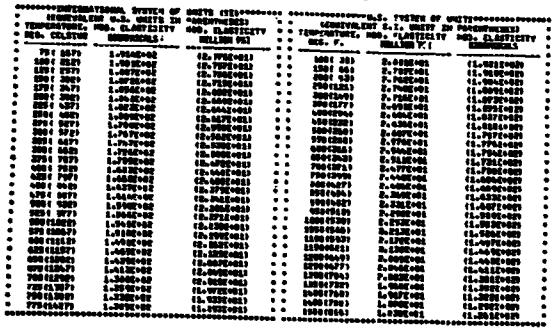

TABLE B-VI

Shear Modulus for Annealed 316 Stainless Steel [14]

1971 ASME CODE

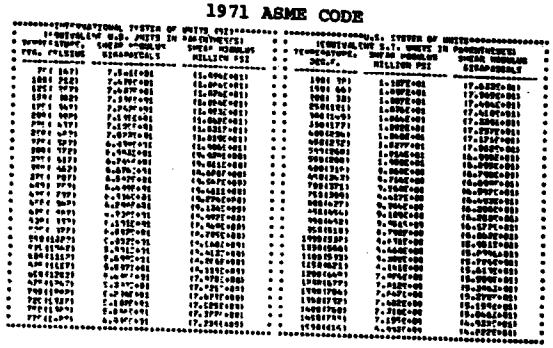

TABLE B-VII

Poisson's Ratio for Annealed 316 Stainless Steel [14]

INTERNATIONAL SYSTEM OF UNITS (SI) (EQUIVALENT U.S. UNITS IN PARENTHESES)		U.S. SYSTEM OF UNITS (EQUIVALENT S.I. UNITS IN PARENTHESES)	
TEMPERATURE, DEG. CELSIUS	POISSON'S RATIO	TEMPERATURE, DEG. F.	POISSON'S RATIO
75 (167)	2.894E-01	100 (38)	2.686E-01
100 (212)	2.717E-01	150 (66)	2.684E-01
125 (257)	2.741E-01	200 (93)	2.711E-01
150 (302)	2.762E-01	250 (121)	2.737E-01
175 (347)	2.784E-01	300 (149)	2.761E-01
200 (392)	2.634E-01	350 (177)	2.785E-01
225 (437)	2.824E-01	400 (204)	2.808E-01
250 (482)	2.844E-01	450 (232)	2.651E-01
275 (527)	2.862E-01	500 (266)	2.851E-01
300 (572)	2.881E-01	550 (288)	2.872E-01
325 (617)	2.899E-01	600 (316)	2.892E-01
350 (662)	2.917E-01	650 (343)	2.912E-01
375 (707)	2.934E-01	700 (371)	2.931E-01
400 (752)	2.951E-01	750 (399)	2.951E-01
425 (797)	2.969E-01	800 (427)	2.976E-01
450 (842)	2.966E-01	850 (454)	2.989E-01
475 (887)	3.003E-01	900 (482)	3.004E-01
500 (932)	3.022E-01	950 (510)	3.027E-01
525 (977)	3.037E-01	1000 (538)	3.046E-01
550 (1022)	3.055E-01	1050 (566)	3.066E-01
575 (1067)	3.072E-01	1100 (593)	3.086E-01
600 (1112)	3.091E-01	1150 (621)	3.106E-01
625 (1157)	3.110E-01	1200 (649)	3.127E-01
650 (1202)	3.122E-01	1250 (677)	3.140E-01
675 (1247)	3.147E-01	1300 (704)	3.171E-01
700 (1292)	3.167E-01	1350 (732)	3.194E-01
725 (1337)	3.184E-01	1400 (760)	3.217E-01
750 (1382)	3.219E-01	1450 (788)	3.242E-01
775 (1427)	3.211E-01	1500 (816)	3.266E-01

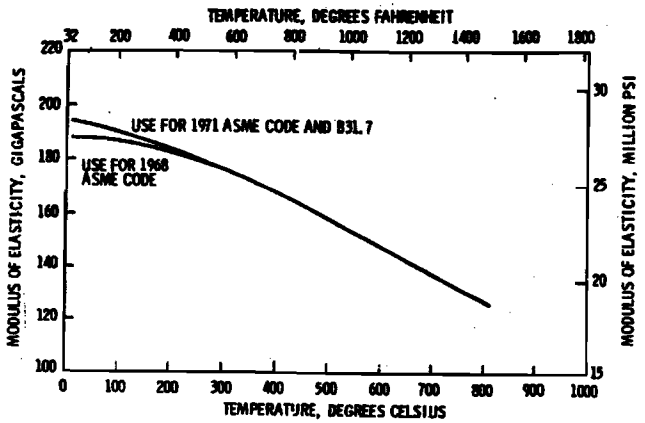

Figure B-1. Young's modulus of 304SS, annealed [14].

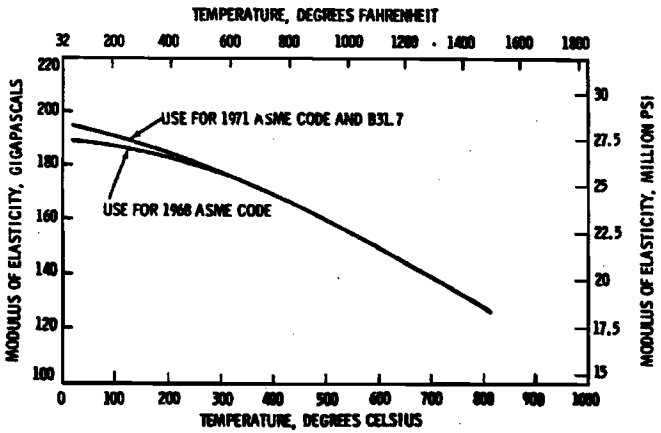

Figure B-2. Young's modulus of 316SS, annealed [14].

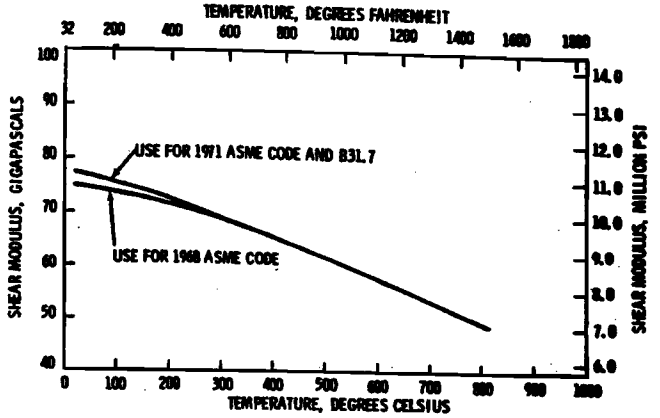

Figure B-3. Shear modulus of 304SS, annealed [14].

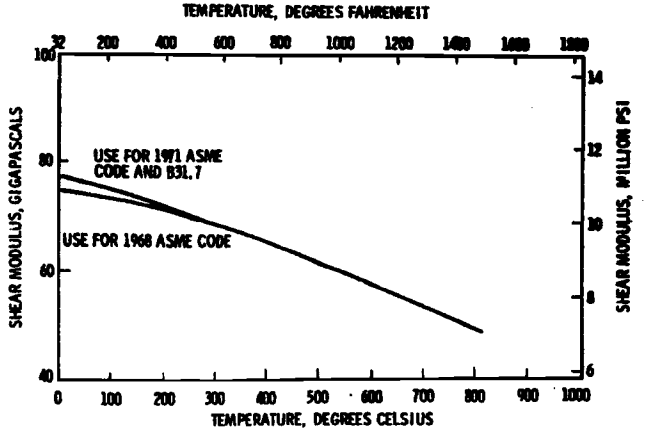

Figure B-4. Shear modulus of 316SS, annealed [14].

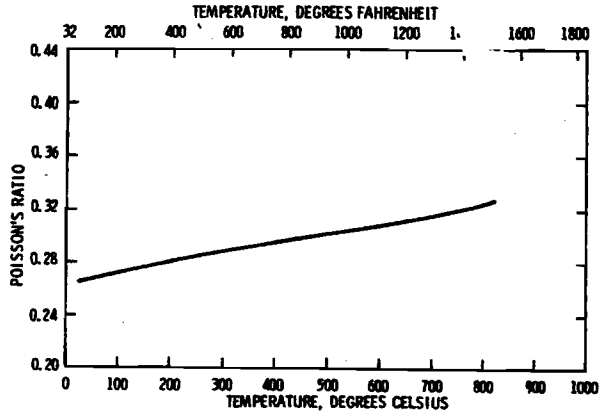

Figure B-5. Poisson's ratio of 304SS, annealed [14].

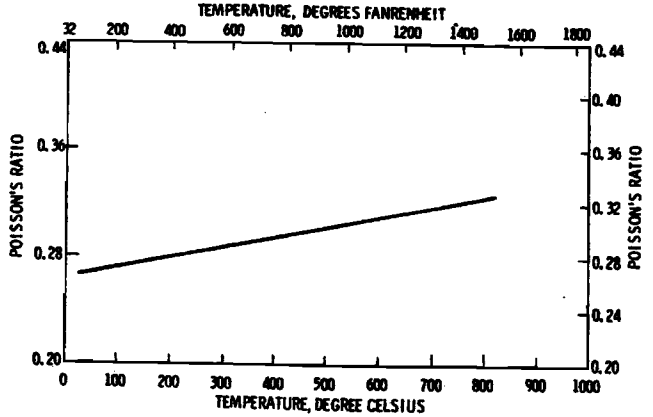

Figure B-6. Poisson's ratio of 316SS, annealed [14].

Uranium

The influence of temperature on the elastic properties of uranium are presented in Table B-VIII and Figure B-7. The solid curve in the latter refers to the modulus of random, non-textured polycrystalline uranium [62], while the minimum and maximum

TABLE B-VIII

Probable Values for Elastic Moduli
of Non-textured Polycrystalline Uranium [64]

Temperature (K)	Young's Modulus (10^6 psi)	Shear Modulus (10^6 psi)	Poisson's Ratio
200	30.5	12.50	0.22
300	29.1	11.80	0.23
400	27.6	11.20	0.23
500	26.1	10.50	0.23
600	24.3	9.70	0.25
700	22.3	8.70	0.28
800	19.7	7.60	0.30

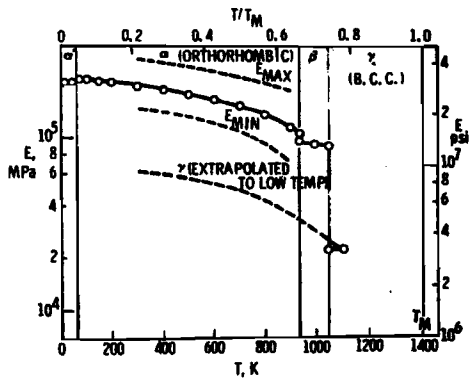

Figure B-7. Young's modulus of pure polycrystalline uranium as a function of temperature. The modulus of non-textured uranium is given by the solid line. The maximum and minimum moduli for alpha uranium from single crystal measurements are also plotted [62, 63].

values were obtained from specifically oriented uranium single crystals [63]. These results show that, whereas the modulus of non-textured polycrystalline uranium at 298 K is 29 x 10^6 psi, it can be as high as 41.5 x 10^6 psi or as low as 21.4 x 10^6 psi for a textured sample.

Finally, the authors were unable to obtain any reliable data on the influence of dilute alloy additions (e.g., 2 weight percent Mo) on the elastic properties of uranium.

Lead

The influence of temperature on the Young's modulus of cast high purity lead is shown in Figure B-8. Again, increasing temperature results in a gradual decrease in modulus. Attempts to locate more complete information, including values of the shear modulus and Poisson's ratio, have been unsuccessful to date.

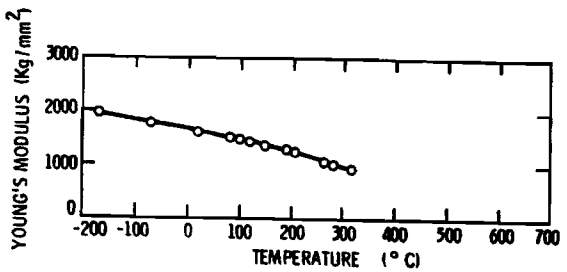

Figure B-8. Young's modulus of lead [65].

APPENDIX C

List of Symbols

σ = true stress

σ_p = proportional limit

ϵ = true plastic strain = ln(1+e)

e = engineering strain = $\Delta l/l_o$

ϵ_L = total true strain

E = Young's modulus

$\Delta L/L_o$ = thermal linear expansion,

L_T = length at temperature T

L_o = length at 293 K

ΔL = $L_T - L_o$

DISTRIBUTION:

U.S. Nuclear Regulatory Commission (242 copies for R7)
Division of Document Control
Distribution Services Branch
7920 Norfolk Avenue
Bethesda, MD 20014

U.S. Nuclear Regulatory Commission (26)
Washington, D. C. 20555
Attn:
W. F. Anderson, OSD
C. R. Chappell, NMSS
R. G. Clary, NMSS
D. J. Guzy, NMSS
M. Hartzman, NRR
V. Hodge,NMSS
W. R. Lahs, RES (10)
W. H. Lake, NMSS
C. E. MacDonald, NMSS (5)
C. R. Marotta, NMSS
J. O. Mayor, NMSS
R. H. Odegaarden, NMSS
C. R. Shieh, NMSS

4400 A. W. Snyder
Attn: D. J. McCloskey, 4410
J. V. Walker, 4420
J. A. Reuscher, 4450
4550 R. M. Jefferson
4551 R. E. Luna
4552 R. B. Pope
4552 G. C. Allen, Jr.
4552 R. G. Eakes
4551 J. M. Freedman
4553 W. A. Von Riesemann (5)
4553 D. L. Wesenberg
5500 O. E. Jones
5520 T. B. Lane
5521 S. W. Key
5521 D. W. Lobitz
5521 C. M. Stone
5522 T. G. Priddy
5800 R. S. Claassen
Attn: R. G. Kepler, 5810
R. L. Schwoebel, 5820
H. Saxton, 5840
5830 M. J. Davis
Attn: M. J. Magnani, 5831
R. W. Rohde, 5832
J. L. Ledman, 5833
D. M. Maddox, 5834
C. Karnes, 5835
5832 J. W Munford
5832 K. Eckelmeyer
5832 H. J. Mack (25)
5833 G. Knorovsky (10)
8120 W. E. Alzheimer
8121 A. Jones
8122 C. S. Hoyle
8123 B. Zinke
8124 A. F. Baker
8310 D. Schuster
Attn: W. R. Hoover, 8314

3141 T. L. Werner (5)
3151 W. L. Garner (3)
For DOE/TIC (Unlimited Release)
3172-3 R. P. Campbell (25)
For DOE/TIC (Unlimited Release)
8266 E. A. Aas